Pergamon

Int. J. Heat Mass Transfer. Vol. 39, No. 6, pp. 1141–1148, 1996

0017–9310/96 $15.00 + 0.00

0017–9310(95)00211–1

Mixed convection from a vertical cylinder embedded in a porous medium : non-Darcy model

T. K. ALDOSS, M. A. JARRAH and B. J. AL-SHA'ER

Mechanical Engineering Department, Jordan University of Science and Technology, P.O. Box 3030, Irbid, Jordan

(*Received* 5 *August* 1994 *and in final form* 20 *June* 1995)

Abstract—The problem of Non-Darcian mixed convection about a vertical cylinder embedded in a porous medium is analyzed. Nonsimilarity solutions are obtained for the case of variable wall temperature (VWT) and variable surface heat flux (VHF).

The entire mixed convection regime is covered by two different nonsimilarity parameters : one for VWT and the other for VHF, including the two limits of pure forced convection and pure free convection. A finite-difference scheme was used to solve the system of the transformed governing equations.

The effect of four characteristic parameters namely the heating condition at the wall, the strength of mixed convection, the inertia and the boundary effect (the non-Darcian effect), and the cylinder curvature effect, on the heat transfer is investigated numerically. The results are found to be in excellent agreement with those of previous work.

1. INTRODUCTION

Convective heat transfer and fluid flow in porous media has recently received considerable attention with geophysical and engineering applications. Such applications include geothermal systems, chemical catalytic reactor, packed sphere beds, grain storage and thermal insulation engineering.

In most of the previous studies the boundary-layer formulation based on Darcy's law was adopted. The no-slip boundary condition is found to modify the velocity profile near the wall which in turn affects the rate of heat transfer from the wall, not considering such effect will result in error in heat transfer calculations. Also, when the Reynolds number is of an order greater than one, the inertial force is no longer negligible compared with the viscous force and must be included. These two effects are incorporated in the present analysis using the non-Darcy model proposed by Brinkman–Forchheimer [1].

Kumari and Nath [2] studied the mixed convection from a thin vertical cylinder embedded in a saturated porous medium. The effect of inertial force is included in their model. Chen *et al.* [3] considered other non-Darcian effects, the no-slip boundary condition, inertial force, variable porosity and thermal dispersion, on mixed convection about an isothermal vertical cylinder in a saturated porous medium. The formulation of Chen *et al.* [3] does not allow calculation of the entire mixed convection regime, since the pure natural convection requires the mixed convection parameter in their formulation (Gr/Re) to go to ∞.

In the present work mixed convection from a vertical cylinder embedded in saturated porous medium is investigated. The non-Darcy model is used to incorporate the effects of the inertial force and no-slip boundary condition. Two wall heating conditions are considered, variable wall temperature (VWT) and variable surface heat flux (VHF). A nonsimilar solution is sought, since in the general nonisothermal heating boundary conditions the similarity solution is not possible. Following Aldoss *et al.* [4] a nonsimilar solution that covers the entire regime of mixed convection from the pure forced convection limit to the pure natural convection limit, is constructed, using a mixed convection parameter which takes values between 1 and 0. The model also includes the effect of the cylinder curvature.

The resulting transformed governing equations are then solved by a finite difference scheme. Numerical results for both variable wall temperature and variable surface heat flux conditions, and the effect of other governing parameters on the Nusselt number are presented.

2. FORMULATIONS

To obtain the volume average conservation equations the following assumptions were made :

(1) The flow is steady, laminar, incompressible and two-dimensional.

(2) The Boussinesq approximation is valid, which is a two-part approximation : (a) it neglects all variable property effects in the three governing equations, except for density in the buoyancy term of momentum

NOMENCLATURE

C_f local friction factor
Da_x local Darcy number, K/x^2
D_p pore or particle diameter [m]
f dimensionless stream function
g acceleration of the gravity [m s^{-2}]
$h(x)$ local heat transfer coefficient [W m^{-2} K^{-1}]
$\bar{h}$ average heat transfer coefficient, $\frac{1}{L}\int_0^L h\,dx$ [W m^{-2} K^{-1}]
k thermal conductivity [W m^{-1} K^{-1}]
K permeability coefficient of the porous medium [m^2]
K' coefficient of Forchheimer's equation
L length of the plate [m]
Nu_x local Nusselt number, hx/k
$\overline{Nu}$ average Nusselt number, $\bar{h}L/k$
Pe_x local Peclet number, $U_\infty x/\alpha$
Pe^* parameter of the wall effect
Pr Prandtl number, ν/α
q_w local surface heat flux [W m^{-2}]
R^* inertial effect parameter $= U_\infty K'/\nu$
Ra_x local Rayleigh number for (VWT) case, $Kg\beta(T_w - T_\infty)x/\nu\alpha$
Ra_x^* modified local Raleigh number for (VHF) case, $Kg\beta g_w x^2/k\nu\alpha$
Re Reynolds number, $U_\infty x/\nu$
T temperature [K]
T_∞ free stream temperature [K]
T_w wall temperature [K]
U velocity component in the x-direction [m s^{-1}]
V velocity component in r-direction [m s^{-1}]
$\vec{V}$ two-dimensional velocity vector [m s^{-1}]
VHF variable surface heat flux boundary condition
VWT variable wall temperature boundary condition
x axial coordinates
r radial coordinate.

Greek symbols
α effective thermal diffusivity of saturated porous medium [m^2 s^{-1}]
β volumetric coefficient of thermal expansion [K^{-1}]
δ boundary layer thickness
η pseudo-similarity variable
θ dimensionless temperature
μ dynamic viscosity [N s m^{-2}]
ν kinematic viscosity [m^2 s^{-1}]
ζ nonsimilarity parameters
ρ density of the fluid [kg m^{-3}]
τ_w local wall shear stress, $\mu\,(\partial u/\partial y)_{y=0}$ [N m^{-2}]
λ curvature parameter
ε porosity
ψ stream function
χ rate of change of ζ with respect to x.

Subscripts
f variable surface heat flux case
t variable wall temperature case
∞ free stream condition
w wall condition.

equations and (b) it approximates the density difference term with a simplified equation of state, that is

$$\rho = \rho_\infty(1-\beta(T-T_\infty)) \tag{1}$$

where β is the volumetric coefficient of thermal expansion.

(3) The fluid and the solid matrix are everywhere in local thermodynamic equilibrium.

(4) The thermophysical properties of the fluid are homogeneous and isotropic.

(5) The temperature of the fluid is everywhere below the boiling point.

Consider a vertical cylinder embedded in a fluid-saturated porous medium, subjected to a combined natural and forced convection heat transfer. Figure 1 shows the physical problem. Two kinds of wall heating conditions are considered, variable wall temperature (VWT), and variable heat flux (VHF). Using the Brinkman–Forchheimer model and under the above mentioned assumptions the governing equations in cylindrical coordinates are:

$$\frac{\partial U}{\partial x} + \frac{1}{r}\frac{\partial (rV)}{\partial r} = 0 \tag{2}$$

$$U + \frac{K'}{\nu}U^2 = \frac{-K}{\mu}\left[\frac{dp}{dx} + \rho g_x - \frac{\mu}{\varepsilon}\left\{\frac{1}{r}\frac{\partial}{\partial r}\left(r\frac{\partial U}{\partial r}\right) + \frac{\partial^2 U}{\partial x^2}\right\}\right] \tag{3}$$

$$V + \frac{K'}{\nu}V^2 = \frac{-K}{\mu}\left[\frac{dp}{dy} + \rho g_r - \frac{\mu}{\varepsilon}\left\{\frac{1}{r}\frac{\partial}{\partial r}\left(r\frac{\partial V}{\partial r}\right) + \frac{\partial^2 V}{\partial x^2}\right\}\right] \tag{4}$$

$$U\frac{\partial T}{\partial x} + V\frac{\partial T}{\partial r} = \alpha\left[\frac{\partial^2 T}{\partial x^2} + \frac{1}{r}\frac{\partial}{\partial r}\left(r\frac{\partial T}{\partial r}\right)\right]. \tag{5}$$

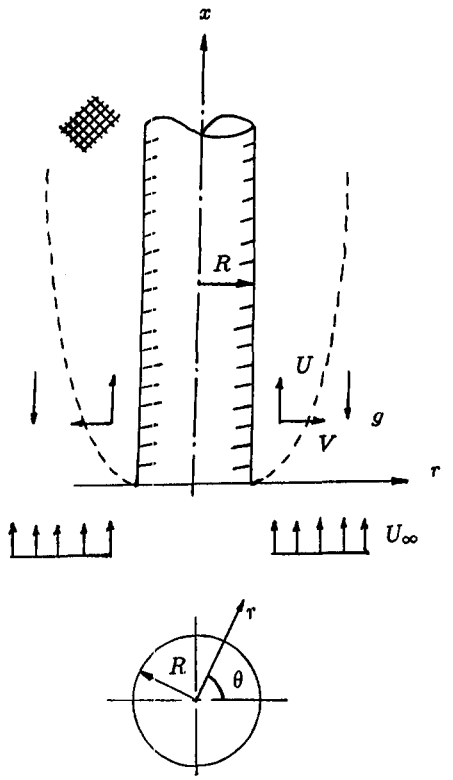

Fig. 1. The physical problem.

In writing the above equations, axisymmetrical flow is considered where x and r are the axial and radial coordinates, and U and V are the axial and radial volume-averaged velocities. The gravitational acceleration (g) is acting downward in a direction opposite to the x-direction, and thus, $g_r = 0$. The non-Darcy effects (inertia and boundary) are introduced through the two terms

$$\left(\frac{K'}{\nu}\vec{V}^2\right)$$

and

$$\frac{\mu}{\varepsilon}\frac{1}{r}\frac{\partial}{\partial r}\left(r\frac{\partial \vec{V}}{\partial r}\right)$$

in the momentum equations, respectively. By introducing the boundary effect term the order of the governing equations is raised by one, which enables applying the no-slip boundary condition at the wall.

The stream function (ψ) defined as:

$$\left.\begin{aligned} U &= \frac{R}{r}\frac{\partial \psi}{\partial r} \\ V &= -\frac{R}{r}\frac{\partial \psi}{\partial x} \end{aligned}\right\} \tag{6}$$

is introduced to satisfy the continuity equation, equation (2), identically, where R is the cylinder radius.

In term of stream function and after applying the boundary layer approximations, equations (3)–(5) become:

$$\frac{\partial}{\partial r}\left(\frac{R}{r}\frac{\partial \psi}{\partial r}\right)+\frac{K'}{\nu}\frac{\partial}{\partial r}\left(\frac{R}{r}\frac{\partial \psi}{\partial r}\right)^2 = \frac{K}{\nu}g\beta\frac{\partial T}{\partial r}+\frac{K}{\varepsilon}\frac{\partial}{\partial r}\left[\frac{1}{r}\frac{\partial}{\partial r}\left\{r\frac{\partial}{\partial r}\left(\frac{R}{r}\frac{\partial \psi}{\partial r}\right)\right\}\right] \tag{7}$$

$$\frac{\partial \psi}{\partial r}\frac{\partial T}{\partial x}-\frac{\partial \psi}{\partial x}\frac{\partial T}{\partial r}=\alpha\left[\frac{1}{r}\frac{\partial}{\partial r}\left(r\frac{\partial T}{\partial r}\right)\right] \tag{8}$$

subjected to the following boundary conditions

(1) Wall thermal condition

(a) Power law variation heat flux at the wall:

$$r = R \Rightarrow q_w = bx^m \tag{9}$$

(b) Power law variation temperature at the wall:

$$r = R \Rightarrow T_w - T_\infty = ax^n \tag{10}$$

(2) No-slip condition at the wall:

$$r = R \Rightarrow \begin{cases} U = 0 \\ V = 0 \end{cases} \tag{11}$$

(3) Free stream velocity outside the boundary layer:

$$r \to \infty \Rightarrow \begin{cases} U = U_\infty \\ \dfrac{\partial U}{\partial r} = 0 \end{cases} \tag{12}$$

(4) Constant temperature outside the thermal boundary layer:

$$r \to \infty \Rightarrow T = T_\infty \tag{13}$$

3. NONSIMILARITY TRANSFORMATION

3.1. *Variable wall temperature (VWT)*: ($T_w - T_\infty = ax^n$)

Modifying the similarity variables introduced by Chen *et al.* [3] the following dimensionless variables are introduced:

$$\eta = \frac{1}{x}Pe_x^{1/2}\zeta_t^{-1}\left(\frac{r^2}{2R}-\frac{R}{2}\right) \tag{14}$$

$$\psi(\zeta_t, \eta) = \alpha Pe_x^{1/2} f(\zeta_t, \eta)\zeta_t^{-1} \tag{15}$$

$$\theta_t(\zeta_t, \eta) = \frac{T - T_\infty}{T_w - T_\infty} \tag{16}$$

$$\zeta_t = \zeta_t(x). \tag{17}$$

In terms of these variables the governing equations and boundary conditions equations (7)–(13) become

$$(1+\lambda\eta\zeta_t)\zeta_t^{-2}Pe^* f^{IV} - \zeta_t^{-2}R^*[f'^2]' - f'' + 2\lambda Pe^*\zeta_t^{-1}f''' = -(\zeta_t - 1)^2\theta_t' \tag{18}$$

$$(1+\lambda\eta\zeta_t)\theta''+[(\tfrac{1}{2}-\chi_t)f+\lambda\zeta_t]\theta'-n\theta f' = -\chi_t\zeta_t\left[\theta_t'\frac{\partial f}{\partial\zeta_t}-f'\frac{\partial\theta_t}{\partial\zeta_t}\right] \quad (19)$$

$$\left.\begin{aligned} f'(0,\zeta_t)&=0 \quad & \theta_t(\infty,\zeta_t)&=0\\ f(0,\zeta_t)&=0 \quad & f'(\infty,\zeta_t)&=\zeta_t^2\\ \theta_t(0,\zeta_t)&=1.0 \quad & f''(\infty,\zeta_t)&=0 \end{aligned}\right\} \quad (20)$$

where

$$\zeta_t=\frac{Pe_x^{1/2}}{Pe_x^{1/2}+Ra_x^{1/2}} \quad (21)$$

$$Pe^*=\frac{Da_xPe_x}{\varepsilon} \quad (22)$$

$$R^*=\frac{K'U_\infty}{\nu} \quad (23)$$

$$\chi_t=\frac{x}{\zeta_t}\frac{\partial\zeta_t}{\partial x}=-\frac{n}{2}(1-\zeta_t) \quad (24)$$

$$Da_x=\frac{K}{x^2} \quad (25)$$

$$Ra_x=\frac{g\beta Kx(T_w-T_\infty)}{\alpha\nu} \quad (26)$$

$$Pe_x=\frac{U_\infty x}{\alpha} \quad (27)$$

$$\lambda=\frac{2}{Pe_x^{1/2}}\frac{x}{R} \quad \text{[the curvature parameter]}. \quad (28)$$

In the above system of equations the prime denotes partial differentiations with respect to η, and ζ_t is the nonsimilar mixed convection parameter for the variable wall temperature case, where $\zeta_t=1$ corresponds to pure forced convection, and $\zeta_t=0$ corresponds to pure free convection. The limit of $\lambda=0$ corresponds to vertical flat plate.

The physical quantities of interest include the velocity components U and V, the local wall shear stress $\tau_w=\mu(\partial U/\partial r)_{r=R}$ and the local Nusselt number $Nu_x=hx/k$ where $h=q_w/(T_w-T_\infty)$ and $q_w=-k(\partial T/\partial r)_{r=R}$. They are given by:

$$U=U_\infty\zeta_t^{-2}f'(\zeta_t,\eta) \quad (29)$$

$$V=\frac{r}{R}\left\{-\frac{\alpha}{x}Pe_x^{1/2}\zeta_t^{-1}\left[(\tfrac{1}{2}-\chi_t)f-(\tfrac{1}{2}+\chi_t)\eta f'+\chi_t\zeta_t\frac{\partial f}{\partial\zeta_t}\right]\right\} \quad (30)$$

$$\tau_w\left(\frac{x^2}{\mu\alpha}\right)[Pe_x^{1/2}+Ra_x^{1/2}]^{-3}=f''(\zeta_t,0) \quad (31)$$

$$Nu_x[Pe_x^{1/2}+Ra_x^{1/2}]^{-1}=-\theta_t'(\zeta_t,0). \quad (32)$$

The average Nusselt number $\overline{Nu}$ can be evaluated by finding the average heat transfer coefficient $\bar{h}$ from the local Nusselt number expression, equation (32). The final expression is:

$$\left(\frac{n}{2}\right)\overline{Nu}Pe_L^{-1/2}=\left(\frac{\zeta_{t_L}}{1-\zeta_{t_L}}\right)^{1/n}\times\int_{\zeta_{t_L}}^{1}\frac{-\theta_t'(\zeta_t,R)}{\zeta_t^3}\left(\frac{1-\zeta_t}{\zeta_t}\right)^{\frac{1-n}{n}}d\zeta_t. \quad (33)$$

For the case of uniform wall temperature (i.e. $n=0$) the corresponding average Nusselt number expression can be written as:

$$\zeta_{t_L}\overline{Nu}[Pe_L^{-1/2}]_{n=0}=-2\theta_t'(\zeta_{t_L},0). \quad (34)$$

3.2. *Variable surface heat flux (VHF)*: ($q_w=bx^m$)

For this case the following dimensionless variables are introduced

$$\eta=\frac{1}{x}Pe_x^{1/2}\zeta_f^{-1}\left(\frac{r^2}{2R}-\frac{R}{2}\right) \quad (35)$$

$$\psi(\zeta_f,\eta)=\alpha Pe_x^{1/2}f(\zeta_f,\eta)\zeta_f^{-1} \quad (36)$$

$$\theta_f(\zeta_f,\eta)=\frac{T-T_\infty}{q_wx/k}Pe_x^{1/2}\zeta_f^{-1} \quad (37)$$

$$\zeta_f=\zeta_f(x). \quad (38)$$

In terms of these variables the governing equations and boundary conditions equations (7)–(13) are transformed into

$$(1+\lambda\eta\zeta_f)\zeta_f^{-2}Pe^*f^{IV}-\zeta_f^{-2}R^*[f'^2]'-f''+2\lambda Pe^*\zeta_f^{-1}f'''+(\zeta_f-1)^3\theta_f'=0 \quad (39)$$

$$(1+\lambda\eta\zeta_f)\theta''+[(\tfrac{1}{2}-\chi_f)f+\lambda\zeta_f]\theta'-n\theta f' = (m+\tfrac{1}{2}+\chi_f)=-\chi_f\zeta_f\left[\theta_f'\frac{\partial f}{\partial\zeta_f}-f'\frac{\partial\theta_f}{\partial\zeta_f}\right] \quad (40)$$

$$\left.\begin{aligned} f'(0,\zeta_f)&=0 \quad & \theta_f(\infty,\zeta_f)&=0\\ f(0,\zeta_f)&=0 \quad & f'(\infty,\zeta_f)&=\zeta_f^2\\ \theta_f'(0,\zeta_f)&=-1.0 \quad & f''(\infty,\zeta_f)&=0 \end{aligned}\right\} \quad (41)$$

where

$$\zeta_f=\frac{Pe_x^{1/2}}{Pe_x^{1/2}+Ra_x^{*1/3}} \quad (42)$$

$$Pe_x^*=\frac{Da_xPe_x}{\varepsilon} \quad (43)$$

$$R^*=\frac{K'U_\infty}{\nu} \quad (44)$$

$$\chi_f=\frac{x}{\zeta_f}\frac{\partial\zeta_f}{\partial x}=-\frac{2m+1}{6}(1-\zeta_f) \quad (45)$$

$$Da_x=\frac{K}{x^2} \quad (46)$$

$$Ra_x^* = \frac{q_w g \beta K x^2}{\alpha \nu k} \tag{47}$$

$$Pe_x = \frac{U_\infty x}{\alpha} \tag{48}$$

$$\lambda = \frac{2}{Pe_x^{1/2}} \frac{x}{R} \quad \text{[the curvature parameter]}. \tag{49}$$

In the above system of equations again the prime denotes partial differentiations with respect to η, and ζ_f is the nonsimilar mixed convection parameter for the variable heat flux case, where $\zeta_f = 1$ corresponds to pure forced convection, and $\zeta_f = 0$ corresponds to pure free convection.

The corresponding physical quantities are given by:

$$U = U_\infty \zeta_f^{-2} f'(\zeta_f, \eta) \tag{50}$$

$$V = -\frac{r}{R}\left\{\frac{\alpha}{x} Pe_x^{1/2} \zeta_f^{-1} \left[\left(\tfrac{1}{2} - \chi_f\right) f - \left(\tfrac{1}{2} + \chi_f\right)\eta f' + \chi_f \zeta_f \frac{\partial f}{\partial \zeta_f}\right]\right\} \tag{51}$$

$$\tau_w \left(\frac{x^2}{\mu\alpha}\right)[Pe_x^{1/2} + Ra_x^{*1/3}]^{-3} = f''(\zeta_f, 0) \tag{52}$$

$$Nu_x[Pe_x^{1/2} + Ra_x^{*1/3}]^{-1} = 1/\theta_f(\zeta_f, 0). \tag{53}$$

The average Nusselt number $\overline{Nu}$ can be obtained from the local Nusselt number expression equation (53). It is:

$$\frac{2m+1}{6} \overline{Nu} Pe_L^{-1/2} = \left(\frac{\zeta_{f_L}}{1-\zeta_{f_L}}\right)^{3/2m+1} \int_{\zeta_{f_L}}^{1} \frac{1/\theta(\zeta_f, R)}{\zeta_f^3} \times \left(\frac{1-\zeta_f}{\zeta_f}\right)^{\frac{2-m}{2m+1}} d\zeta_f. \tag{54}$$

For the case of uniform wall temperature, (i.e. $m = -0.5$), equation (54) reduces to

$$\overline{Nu}|_{m=-0.5} = \frac{2Pe_L}{\theta(\zeta_{f_L}, 0)} \zeta_{f_L}^{-1} \tag{55}$$

The transformed governing equations and the corresponding boundary conditions, equations (18)–(28), for VWT case and (39)–(49) for VHF case are then solved using Keller–Box method [5].

The rate of convergence depends on the previous iteration (initial guess), so convergence can be easily obtained provided that the initial estimates to desired solution are close enough. In this work, the values at the previous station (ζ^{n-1}) were used as initial estimates to the present station (ζ^n).

Different $\Delta\eta$ spacing (0.01, 0.05, ..., 0.5) and $\Delta\zeta$ steps (0.01, 0.05 and 0.1) were tested, and the calculations showed that the rate of convergence of the solution was quadratic in all cases, except when $\Delta\zeta = 0.1$, where the convergence was linear.

Although a uniform grid across the shear layer was quite satisfactory for the most cases, especially in laminar flow, the Keller–Box scheme is unique in that various spacing in both ζ and η direction can be used. In this work, reducing the values of $\Delta\zeta$ and $\Delta\eta$ below 0.05 would result in no changes in the results.

Two types of tests were made in determining the value of η_∞, one with the momentum boundary layer thickness, and the other with the thermal boundary layer thickness. The final value of η_∞ was chosen as so that beyond it the convergence of the solution would not change significantly and the change in the temperature at the edge of it is not significant, i.e. $|\Delta T|_{\eta\infty} < \varepsilon$, where ε was chosen to be 10^{-5}.

Using the single nonsimilar parameter (ζ), where $\zeta = 0$ corresponds to pure free convection and $\zeta = 1$ corresponds to pure forced convection, one needs to run the solution from $\zeta = 0$ to $\zeta = 1$ to cover the whole regime of mixed convection, thus both the computer time and efforts were minimized.

4. RESULTS AND DISCUSSIONS

The effects of all parameters included in the final system on the velocity profile, temperature profile, rate of heat transfer and the local wall shear stress were computed and presented for both Darcian and non-Darcian models. The details are found in [6]. For brevity only their effects on the local Nusselt number are presented here.

4.1. *Effect of the heating condition*

Numerical results were obtained and presented for VWT and VHF wall heating conditions. These results cover the values of the exponent (n) and (m) which are physically realistic. The physically realistic values of these exponents are the ones associated with increased or fixed values of δ and U, the boundary layer thickness and the stream wise velocity component with respect to x as long as the wall temperature at $x > 0$ is different from that of the surrounding. For the vertical cylinder (and the vertical plate), the range of the exponents n and m are $0 \leqslant n \leqslant 1$ and $-0.5 \leqslant m \leqslant 1$

Figures 2 and 3 show the effect of n and m on the local Nusselt number for VWT and VHF cases, respectively.

At higher values of n and m, the thermal boundary layer thickness is smaller and the temperature gradient at the surface is higher. This means that higher values of heat transfer rates (higher Nusselt numbers) are associated with higher values of n and m.

4.2. *Effect of the inertial force*

The parameter $R^* = U_\infty K'/\nu$ is found to characterize the effect of the inertial force, where the inertia term K' is proportional to pore diameter. Therefore, the inertia effects depend strongly on the pore size.

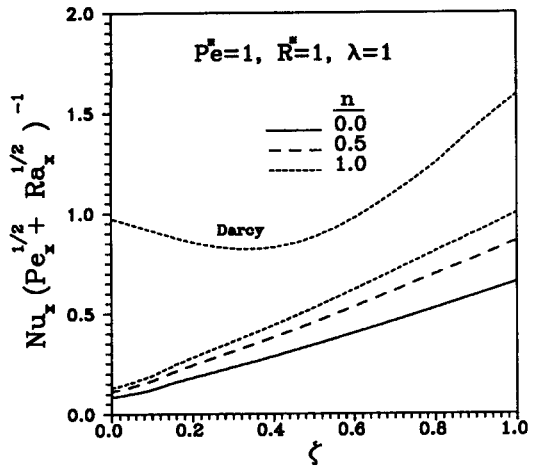

Fig. 2. Local Nusselt number at selected values of n (VWT).

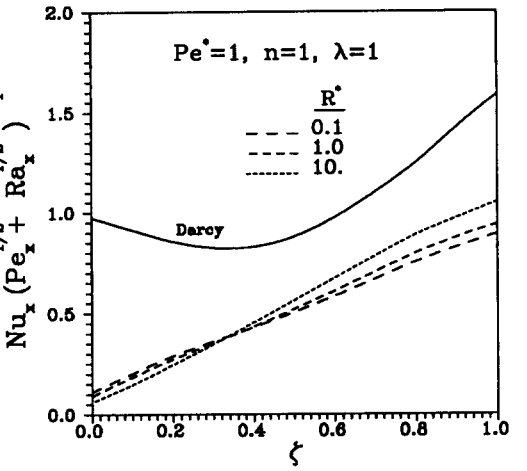

Fig. 4. Local Nusselt number at selected values of R^* (VWT).

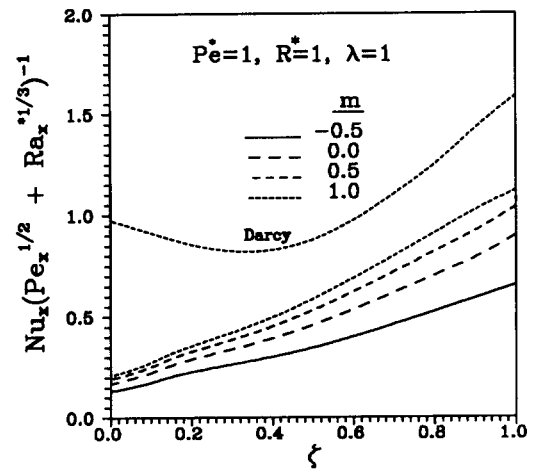

Fig. 3. Local Nusselt number at selected values of m (VHF).

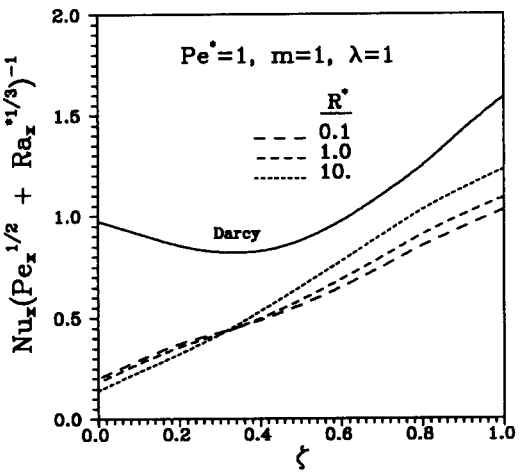

Fig. 5. Local Nusselt number at selected values of R^* (VHF).

For porous media with small pores and low porosities, the permeability is small, and thus, shows negligible inertial effects. On the other hand, for porous media with large pores and porosities, R^* can be quite large, even for normal temperature difference for the same geometry.

Since in actual applications U_∞ can be assumed to be of order one O(1), $\nu = O(10^{-4})$ and $K' = O(10^{-7})$, the parameter R^* becomes O(0.001), so that the value of R^* (0, 1, 10) is enough to test the effect of inertia.

The inertial effect on local Nusselt number is shown in Figs. 4 and 5. Increasing the inertia parameter R^* decreases the rate of heat transfer in the NCDR, and increases it in the FCDR, both in VWT and VHF cases.

4.3. *Effect of boundary*

The parameter

$$Pe^* = \frac{1}{\varepsilon}\frac{U_\infty x}{\alpha}\frac{K}{x^2}$$

is found to characterize the boundary effect, and its physical value, according to Kaviany [7], is of the order (10^{-5}), based on the fact that K is of the order (10^{-12}) and ε is of the order (1).

Pe^* is inversely proportion to x, thus the wall effect will be more pronounced near the leading edge, where the boundary layer solutions are not valid. For low porosity media, the no-slip condition term has strong effects for large temperature difference.

The effects of Pe^* are presented in Figs. 6 and 7. It is clear that as the wall effect parameter increases, the thermal boundary layer thickness increases, resulting in lower heat transfer rate. This is correct for both cases of VWT and VHF, and for the entire mixed convection regime. Moreover, increasing the boundary parameter results in a reduction in the velocity and the velocity gradient within the boundary layer, and thus lowers the local wall shear stress. Details can be found in [6].

4.4. *Effect of curvature*

The curvature effect in the case of a vertical cylinder is introduced by the parameter

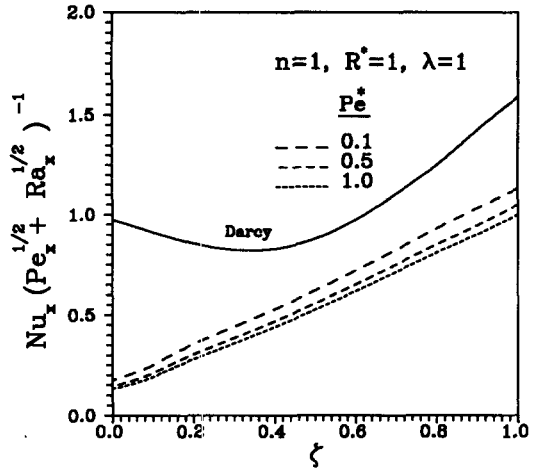

Fig. 6. Local Nusselt number at selected values of Pe^* (VWT).

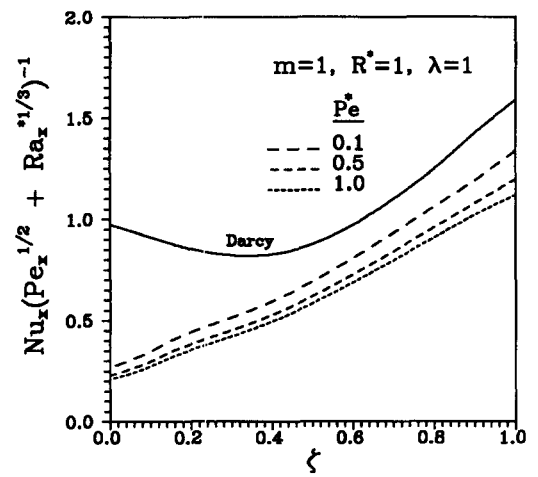

Fig. 7. Local Nusselt number at selected values of Pe^* (VHF).

$$\lambda = \frac{2}{Pe_x^{1/2}} \frac{x}{R}$$

where R is the radius of the cylinder.

The physical value of λ depends on R and Pe_x. Since R must be small compared to x for the assumption of infinite cylinder to be valid with boundary layer approximation (for $x > 0$), the parameter λ is O(0.1).

Figures 8 and 9 show the effect of the curvature parameter (λ) on the local Nusselt number for VWT and VHF, respectively. Increasing λ has the effect of increasing the gradient of the thermal boundary layer at the wall, thus increasing the rate of heat transfer (local Nusselt number). This is prevailing for the entire mixed convection regime. Such an effect of cylinder curvature on the local Nusselt number is found and reported by Gill *et al.* [8]. Since λ has in its definition Pe_x, it is not appropriate as a curvature parameter in the case of pure natural convection. The effect of cylinder curvature in case of pure natural convection is reported by Minkowycz and Cheng [9],

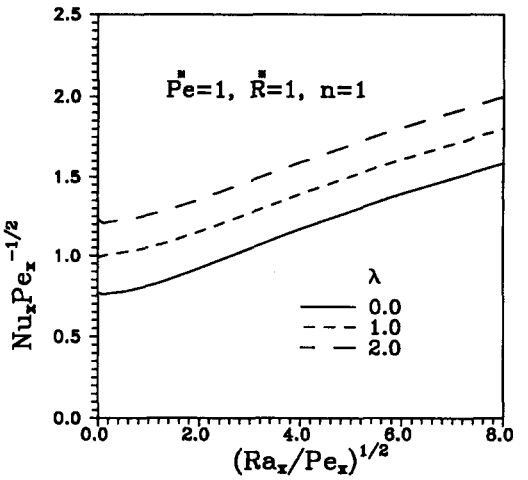

Fig. 8. Local Nusselt number at selected values of λ (VWT).

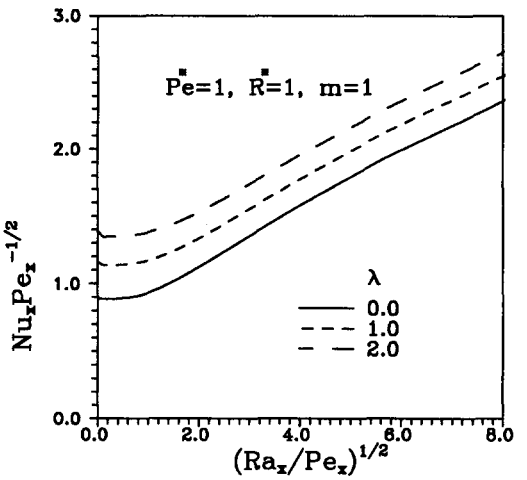

Fig. 9. Local Nusselt number at selected values of λ (VHF).

increasing curvature parameter has the effect of increasing Nu_x.

4.5. *Effect of the strength of mixed convection*

The nonsimilarity parameter ζ measures the strength of mixed convection, where the limit $\zeta = 0$ corresponds to pure natural convection while the other limit $\zeta = 1$ corresponds to pure forced convection. Thus, the values of ζ from 0 to 1 cover all the possible strength of mixed convection including free and forced convections. The effect of ζ on Nu_x is demonstrated in Figs. 2–9. Increasing ζ increases the Nusselt number expression continuously, with the highest value at $\zeta = 1$ (the pure forced convection limit). The behavior of Nu_x with ζ in non-Darcian model is very much different from that of Darcy model. The values of Nu_x are always less in non-Darcian model.

4.6. *Validity*

For the vertical cylinder, the Darcian mixed convection (R^*, Pe^*) with the limit $\lambda = 0$ reduces to a

Darcian mixed convection over a vertical flat plate, a case which was studied by Hsieh *et al.* [10]. Their results could be obtained using the present formulation within 2% accuracy.

Also, the case of non-Darcian effects on mixed convection about a vertical isothermal cylinder embedded in a saturated porous medium was considered by Chen *et al.* [3], the results using the present formulation are compared with their results for the case of pure forced convection with no dispersion nor variable porosity effect. The matching between the two sets of results is found to agree within a tolerance less than 5%.

5. CONCLUSIONS

The mixed convection along a vertical cylinder embedded in a saturated porous medium could be formulated to cover the entire regime of mixed convection with one nonsimilar variable, within the range $\zeta = 1$ for pure forced convection and $\zeta = 0$ for pure free convection, considering two types of heating conditions at the wall VWT and VHF.

Non-Darcian model results are found to be much different than those obtained using Darcian model alone. A boundary parameter has the effect of reducing Nu in the entire mixed convection regime, while the inertia parameter decreases Nu in NCDR and increases it in FCDR.

Larger values of the curvature parameter (lower cylinder radius) has higher values of Nu.

REFERENCES

1. D. A. Nield, The limitations of the Brinkman–Forchheimer equation in modeling flow in a saturated porous medium at an interface, *Int. J. Heat Fluid Flow* **12,** 269–272 (1991).
2. M. Kumari and G. Nath, Non-Darcian mixed convection boundary layer flow on a vertical cylinder in a saturated porous medium, *Int. J. Heat Mass Transfer* **32,** 183–187 (1989).
3. Cha'o-Kuang Chen, Chien-Hsin Chen, W. J. Minkowycz and U. S. Gill, Non-Darcian effects on mixed convection about a vertical cylinder embedded in a saturated porous medium, *Int. J. Heat Mass Transfer* **35,** 3041–3046 (1992).
4. T. K. Aldoss, T. S. Chen and B. F. Armaly, Nonsimilarity solution from horizontal surfaces in a porous medium—Variable wall temperature, *Int. J. Heat Mass Transfer* **36,** 471–477 (1993).
5. T. Cebeci, and P. Bradshaw, *Momentum Transfer in Boundary Layers*, Chaps. 7 and 8. Hemisphere, Washington, D.C. (1977).
6. B. J. Alsha'er, Generalized solution for mixed convection from surfaces embedded in porous media; the entire regime, M.Sc. Thesis, Jordan University of Science and Technology (1994).
7. M. Kaviany, *Principles of Heat Transfer in Porous Media*, Chaps. 1 and 2. Springer, Berlin (1991).
8. U. S. Gill, W. J. Minkowycz, Ch'o-Kuang Chen and Chien-Hsin Chen, Boundary and inertia effects on conjugate mixed convection–conduction heat transfer from a vertical cylindrical fin embedded in a porous medium, *Numer. Heat Transfer* **21,** 423–441 (1992).
9. W. J. Minkowycz and P. Cheng, Free convection about a vertical cylinder embedded in a porous medium, *Int. J. Heat Mass Transfer* **19,** 805–813 (1976).
10. J. C. Hsieh, T. S. Chen and B. F. Armaly, Mixed convection along vertical flat plate embedded in a porous medium: The entire regime, *Int. J. Heat Mass Transfer* **36,** 1819–1825 (1993).